High-Frequency EPR Spectra of $[Fe_8O_2(OH)_{12}(tacn)_6]Br_8$: A Critical Appraisal of the Barrier for the Reorientation of the Magnetization in Single-Molecule Magnets

Anne Laure Barra,[b] Dante Gatteschi,*[a] and Roberta Sessoli[a]

Abstract: A detailed multifrequency high-field–high-frequency EPR (95–285 GHz) study has been performed on the single-molecule magnet of formula $[Fe_8O_2(OH)_{12}(tacn)_6]Br_8 \cdot 9H_2O$, in which tacn = 1,4,7-triazacyclononane. Polycrystalline powder spectra have allowed the estimation of the zero-field splitting parameters up to fourth order terms. The single-crystal spectra have provided the principal directions of the magnetic anisotropy of the cluster. These results have been compared with an evaluation of the intra-cluster dipolar contribution to the magnetic anisotropy; this suggests that single-ion anisotropy is the main contributor to the magnetic anisotropy. The role of the transverse magnetic anisotropy in determining the height of the barrier for the reversal of the magnetization is also discussed.

Keywords: cluster compounds · EPR spectroscopy · magnetic properties

Introduction

Metal-ion clusters whose magnetization relaxes slowly at low temperature have been named single-molecule magnets.[1–6] The meaning of this somewhat emphatic definition is that their behavior is quite similar to that of superparamagnets. These are small, single-domain particles of bulk magnets characterized by magnetic anisotropy comparable with thermal energy. At high temperature the magnetization freely oscillates, and particles behave like paramagnets with a giant-sized magnetic moment. Below a blocking temperature, T_B, the magnetization is trapped in one orientation because the thermal energy is no longer sufficient to allow free rotation. T_B depends on the experimental technique.[7] The magnetization of the single-molecule magnets relaxes very slowly and gives rise to a hysteresis cycle, which makes them bistable.[8] This is an appealing feature, since it may enable the storage of information in one molecule. A further feature of these molecules is that they give rise to several quantum size effects, of which quantum tunneling of the magnetization, QTM, is now one of the most interesting.[9] These materials are currently considered for use in quantum computing devices.

[a] Prof. Dr. D. Gatteschi, Dr. R. Sessoli
Dipartimento di Chimica
Università degli Studi di Firenze
Via Maragliano 77, 50144, Firenze (Italy)
Fax: (+39) 055-354845
E-mail: gattesch@chim1.unifi.it

[b] Dr. A. L. Barra
High Magnetic Field Laboratory
CNRS, 38054 Grenoble (France)

The single-molecule magnets described so far range from $[Mn_{12}O_{12}(RCOO)_{16}(H_2O)_4]$ (Mn_{12}),[10–15] in which the derivative with $R = CH_3$ is the first single-molecule magnet reported,[16] to $[Fe_8O_2(OH)_{12}(tacn)_6]Br_8 \cdot 9H_2O$,[17, 18] ($Fe_8$), in which tacn = 1,4,7-triazacyclononane, to $CrNi_6$ and $CrMn_6$,[19, 20] Mn_4,[5, 21] Mn_7,[22] Fe_4,[6] and Mn_{10}.[23] The list is continuously growing. The highest blocking temperature so far reported is that of Mn_{12}, and this material gives a hysteresis cycle at relatively high temperature. The stepped shape of the hysteresis of oriented crystals[24, 25] is now agreed to indicate the presence of thermally assisted quantum-tunneling effects. Mn_{12} has a ground $S = 10$ state and an Ising type magnetic anisotropy.[25] This means that at low temperature the $M = \pm 10$ states are the only populated ones. If the system is prepared by saturating in a field then only $M = -10$ is populated. When the field is decreased, the return to thermal equilibrium, that is, the equalization of the populations of the $M = +10$ and -10 states, can occur by a thermally activated process. In this case the system must climb the ladder of M states, jumping one rung at a time, passing from $M = -10$ to $M = -9$, then to $M = -8$, and so on. In an early interpretation of the magnetic properties of Mn_{12},[26] it was assumed that the ladder of levels should be climbed up to the highest rung, $M = 0$. The energies of the states are, to a good approximation, given by Equation (1), in which D has been experimentally

$$E(M) = D M^2 \quad (1)$$

determined as $D = 0.5(1)\ cm^{-1}$. The barrier to invert the magnetization was consequently estimated as $\Delta = 100\,|D|$. However, the system can also avoid climbing rung-by-rung up

  0947-6539/00/0609-1608 $ 17.50+.50/0 *Chem. Eur. J.* **2000**, *6*, No. 9

to $M=0$, and can alternatively find a short-cut by tunneling from the state $-M$ to $+M+n$, for which n is an appropriate integer, provided there is a matrix element connecting these two states. In other words, if a transverse anisotropy is present, the relaxation of the magnetization may be accelerated when pairs of levels have the same energy. This corresponds to a quantum-tunneling process.

In order to design new single-molecule magnets the requirements are: i) a large spin ground state, and ii) a large Ising type magnetic anisotropy in the ground state. Further, if one wants to observe large QTM, a large transverse magnetic anisotropy must be present. It must be stressed that the first two points are needed if one aims for a high blocking temperature T_B, but the presence of the transverse anisotropy may effectively quench T_B. Therefore the strategies for high T_B and large QTM are not coincident. As an example, the first two points are very well met by Mn_{12}, but the third is not. Mn_{12}, which has tetragonal symmetry and a large Ising magnetic anisotropy, has a blocking temperature of about 10 K for alternating current (ac) susceptibility measurements, but the tunneling effects have been observed only in the thermally activated regime, and no genuine proof of tunneling between the $M=\pm 10$ states has ever been produced.

Compound Fe_8 has the structure sketched in Figure 1.[17] It has a ground $S=10$ state, like that of Mn_{12}, and an Ising type magnetic anisotropy. The Ising type magnetic anisotropy is

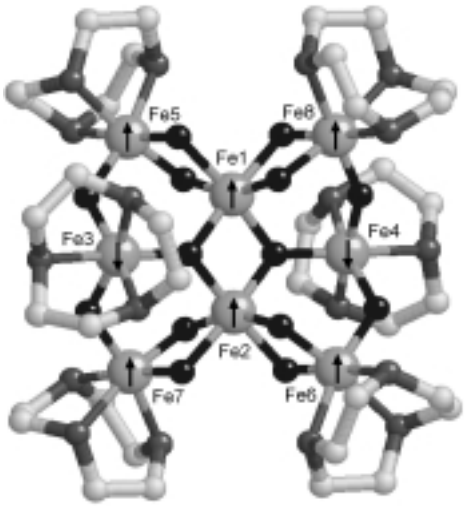

Figure 1. Schematic view of the structure of the $[Fe_8O_2(OH)_{12}(tacn)_6]^{8+}$ cluster. The oxygen atoms are shown in black, nitrogen atoms in gray, and the carbon atoms in white. The arrows represent the spin structure of the ground state as experimentally determined in ref. [49].

about ⅓ that of Mn_{12}, but Fe_8 also has a sizeable transverse magnetic anisotropy, which was originally determined through polycrystalline powder EPR spectra[18] and inelastic neutron-scattering experiments.[27] In agreement with the smaller magnetic anisotropy, the ac blocking temperature is only 3 K. However, the relaxation time of the magnetization becomes independent of temperature below 360 mK.[28] This is so far the best direct example of quantum tunneling of the magnetization in molecular clusters. Furthermore, Fe_8 has been reported to show a periodical dependence of the tunnel splitting on the magnetic field applied along the hard axis. This was the first observation of the so-called Berry phase in magnets.[29]

In order to pave the road to successfully design and synthesize new single molecule magnets it is necessary to accurately define the factors that determine the magnetic anisotropy, both axial and transverse, of the magnetization and to appraise the factors which determine the height of the barrier for the reorientation of the magnetization at low temperature. We have been able to grow single crystals of Fe_8 suitable for single-crystal EPR studies and will analyze in detail the spectra that we recorded in the frequency range 95–285 GHz. High-field high-frequency EPR spectra have indeed been widely used to determine the anisotropy of large molecular clusters.[21, 30, 31] In particular we aim to show the interplay of axial and transverse anisotropy in the determination of the observed relaxation of the magnetization and to provide useful hints for defining the barrier for the reorientation of the magnetization in single-molecule magnets.

Experimental Section

Single crystals (at most ca. 2 mm^3) of Fe_8 were synthesized as previously described.[17] The faces of the crystals were identified on a CAD4 Enraf Nonius four circle X-ray diffractometer. HF-EPR spectra were recorded on a home-made spectrometer[32] operating in the single-pass transmission mode. The main magnetic field was supplied by a superconducting magnet (Cryogenics Consultants) with a maximum field of 12 T. Gunn-diodes and their multipliers (Radiometer Physics) were used as frequency sources, with a basic frequency of 95 GHz or 115 GHz.

Results

Polycrystalline powder spectra: Powder spectra, obtained from a polycrystalline sample pressed into a pellet in order to avoid orientation effects, were recorded at 95, 115, 190, 230, 245, and 285 GHz and at several temperatures ranging from 1.5 K to 35 K. Owing to the large anisotropy of the system complete spectra were obtained only for the 190 and 230 GHz frequencies. The spectra recorded at 190 GHz are shown in Figure 2. At 5 K the features belonging to the three principal directions are well separated from each other. The signals corresponding to the magnetic field applied parallel to the

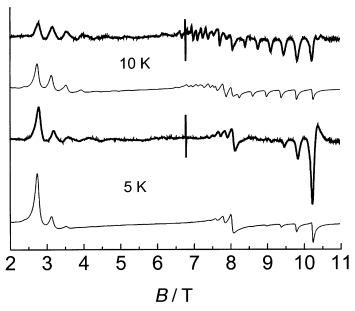

Figure 2. Experimental (bold) and calculated spectra recorded on a pellet of Fe_8 at 189.9540 GHz. Upper curve at $T=10$ K; lower curve at $T=5$ K. A small DPPH marker was added for field calibration. The calculated spectra are obtained with the parameters reported in the text.

  0947-6539/00/0609-1609 $ 17.50+.50/0

easy axis of the system are found at low field, the first one being close to 3 T. Those corresponding to the hard axis are at high field, with the last one close to 10.5 T. The signals found between the 1,1-diphenyl-2-picrylhydrazyl (DPPH) reference and 8.2 T correspond to the third principal axis. At high frequency only the lowest M levels of the spin multiplet are thermally populated at 5 K; this results in a large increase of the signals at the extremes of the spectrum even if these lines have the lowest oscillator strength. When the temperature increases more lines are visible and the intensity pattern changes in proportion to the thermal population and to the transition probability. For the lower frequencies, 95 GHz (reported in Figure 3) and 115 GHz, it is necessary to go to temperatures lower than 5 K to obtain a large polarization effect. In particular the low field signals disappear because they correspond to transitions from excited M levels.

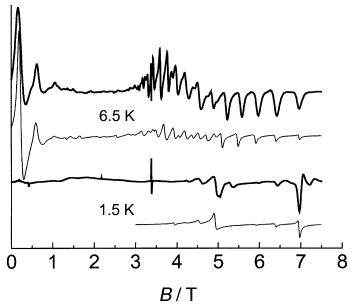

Figure 3. Experimental (bold) and calculated spectra recorded on a pellet of Fe_8 at 94.9770 GHz. Upper curve at $T=6.5$ K; lower curve at $T=1.5$ K. A small DPPH marker was added for field calibration. The calculated spectra are obtained with $g_x=g_y=g_z=2.00$, $D=-0.205\ cm^{-1}$, $E=0.038\ cm^{-1}$, $B_4^0=1.6\times10^{-6}\ cm^{-1}$, $B_4^2=-5\times10^{-6}\ cm^{-1}$, $B_4^4=-8\times10^{-6}\ cm^{-1}$.

Single crystal spectra: The main aims of the single-crystal study were to determine the principal axes of the magnetic anisotropy tensor and to obtain, with higher precision, the zero-field splitting parameters. The latter goal proved very difficult to achieve, especially because of the enormous sensitivity of the spectrum to the exact orientation when close to the hard axis: a rotation by 1° results in dramatic changes to the spectra.

The single-crystal spectra were recorded on quite large crystals of a few cubic millimeters. Several crystals were used, but only one at a time. They were glued with grease and an additional amount of grease was used to cover them in order to reduce the interference with the exciting light. Indeed, at the lowest wavelengths, these parasitic effects are more and more important, particularly at the lowest temperatures. A goniometer mount is not available for our high-frequency EPR spectrometer, so the crystal was oriented by using appropriate supports. The easy and hard axes were determined by using the powder spectra as references, and the intermediate axis was chosen to be perpendicular to the other two. The spectra obtained at 190 GHz for the easy and hard axes are depicted in Figures 4 and 5, respectively. At the lowest temperatures only few lines are visible, corresponding to transitions involving the lowest lying levels. This is a well-known feature of high-field EPR experiments because the

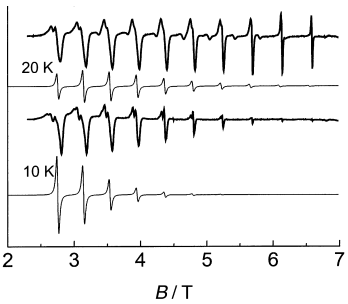

Figure 4. Experimental (bold) and calculated spectra of a single crystal at 189.9541 GHz, with the main magnetic field parallel to the easy axis. The calculated spectra are obtained with the parameters determined from the powder study.

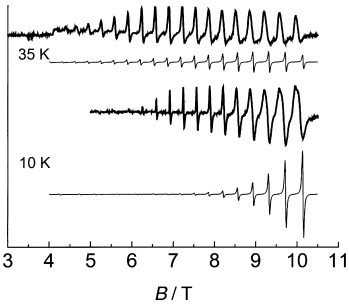

Figure 5. Experimental (bold) and calculated spectra of a single crystal at 189.954 GHz, with the main magnetic field close to the hard axis. The calculated spectra are obtained with the parameters determined from the powder study, and with an angle of 3° between the main magnetic field and the hard axis.

Zeeman energy becomes comparable to kT at low temperature. The depopulation effect can be used to obtain the sign of the zero-field splitting parameters. As the temperature is increased, more resonances are visible as more levels are thermally populated. The intensity pattern shows that the linewidths of the transitions increase towards the extreme of the spectra. This means that the transitions involving states with large M are broader than those with small M. The linewidths approximately scale as M^2. This is an indication of a small distribution of the zero-field splitting parameters' D_i values in the crystal (where i denotes the principal axes x, y or z), an effect similar to the so-called g strain.

Discussion

Fitting of the spectra: The parameters that describe the $S=10$ ground state up to the fourth order are so numerous that a multifrequency study is required. We used a simulation program that performs the exact diagonalization of the hamiltonian for each sampled magnetic field.[33, 34] A first attempt was made with the values determined by the inelastic neutron-scattering measurements with the addition of plausible g values. Whereas the easy axis transitions are well reproduced, those of the intermediate and hard axes do not well agree with the measurements. This part of the spectrum is indeed particularly difficult to reproduce and a really good simulation was not obtained in the frame of a simple $S=10$ picture. In order to restrict the number of parameters and as a

0947-6539/00/0609-1610 $ 17.50+.50/0 Chem. Eur. J. 2000, 6, No. 9

result of the quasi planarity of the magnetic core, the local symmetry of the cluster was approximated to D_2. The spin Hamiltonian is shown in Equation (2).

$$H=\mu_B \boldsymbol{S}\cdot g\cdot B\cdot + D\boldsymbol{S}_z^2 + E(\boldsymbol{S}_x^2-\boldsymbol{S}_y^2) + B_4^0\boldsymbol{O}_4^0 + B_4^2\boldsymbol{O}_4^2 + B_4^4\boldsymbol{O}_4^4 \quad (2)$$

$$\boldsymbol{O}_4^0 = 35\boldsymbol{S}_z^4 - 30S(S+1)\boldsymbol{S}_z^2 + 25\boldsymbol{S}_z^2,$$

$$\boldsymbol{O}_4^2 = \{(7\boldsymbol{S}_z^2 - S(S+1) - 5)(\boldsymbol{S}_+^2 + \boldsymbol{S}_-^2) + (\boldsymbol{S}_+^2 + \boldsymbol{S}_-^2)(7\boldsymbol{S}_z^2 - S(S+1) - 5)\}/4$$

$$\boldsymbol{O}_4^4 = (\boldsymbol{S}_+^4 + \boldsymbol{S}_-^4)/2.$$

In this scheme, two parameters are needed to describe the anisotropy at the second order, namely the usual D and E parameters. Three fourth-order parameters are present, namely B_4^0, B_4^2, and B_4^4. Taking into account the five fourth-order parameters would have modified the numerical values for these terms, but would have not fundamentally changed the calculated spectra.

The best fit for the complete set of spectra was obtained with: $g_x = g_y = g_z = 2.00$, $D = -0.205\ \mathrm{cm}^{-1}$, $E = 0.038\ \mathrm{cm}^{-1}$, $B_4^0 = 1.6\times10^{-6}\ \mathrm{cm}^{-1}$, $B_4^2 = -5\times10^{-6}\ \mathrm{cm}^{-1}$, and $B_4^4 = -8\times10^{-6}\ \mathrm{cm}^{-1}$. The errors and the correlation between the parameters will be discussed below. The simulated powder and single-crystal spectra are depicted together with the experimental ones in Figures 2, 3, 4, and 5. As expected for a cluster that contains ^{6}S iron(III) ions, g is isotropic and equal to 2.0. The D value is higher than the one determined from the first HF-EPR study,[18] as here the multifrequency measurements showed that the g_z value had to be reduced relative to the previously reported value. The D value is thus closer to the one obtained from the inelastic neutron-scattering measurements.[27] The uncertainty in the D value is $\Delta D = \pm 0.004\ \mathrm{cm}^{-1}$. This uncertainty in itself is not that large, but it implies large correlated changes on the other parameters, particularly on the B_4^n terms. For example, $B_4^0 = 0$ for $D = -0.197\ \mathrm{cm}^{-1}$. As a result of the strong correlation, more than one set of parameters reproduce the experimental behavior. A simulation of similar quality has been achieved by using $D = -0.201\ \mathrm{cm}^{-1}$, $E = 0.038\ \mathrm{cm}^{-1}$, $B_4^0 = 5\times10^{-7}\ \mathrm{cm}^{-1}$, $B_4^2 = -7\times10^{-6}\ \mathrm{cm}^{-1}$, and $B_4^4 = 7\times10^{-6}\ \mathrm{cm}^{-1}$. However, this second set seems less probable. Recent experiments have in fact shown that the energy difference between the $M = \pm 10$ of the ground doublet, the so-called tunnel splitting, oscillates with a period of about 0.4 Twhen the external field is applied along the hard axis.[29] We have calculated the field dependence of the tunnel splitting and found that the first set of parameters gives a period of 0.32 T, while the second one gives a period of 0.22 T, which deviates even more from the experimental value.

In the simulation of the spectra, the main difficulty lies in the discrepancies observed in the high-field part of the spectra; indeed, it is not possible to reproduce the splitting between consecutive lines of the x or y orientations together with the position of the two sets of lines. As the fourth-order terms influence the position of the last lines of each set, this flaw cannot be corrected by the consideration of the other two parameters. At this stage, it is difficult to determine with certainty why this is so, but an explanation could be that the single-spin model is not that good, that is, the strong coupling limit is not met. In fact the energy of the first excited $S = 9$ level is not directly known, but the results of the calculations to be described below, suggest a gap of approximately 25 cm^{-1}. Under these conditions the strong exchange limit is not fully achieved and an admixture of M states belonging to the two S states can occur. Notwithstanding these limitations the single-crystal EPR spectra do provide unique information on the magnetic anisotropy of the system.

From these measurements the direction of the principal axes of the anisotropy tensor of the cluster are unambiguously determined with respect to the molecule. The intermediate axis is found to coincide, within the precision of the measurement, with the direction defined by two iron atoms, Fe1 and Fe2, which is a pseudo C_2 symmetry axis for the molecule.[35] Conversely, the two other principal axes do not correspond to a direction defined by iron atoms. The hard axis is found to make an angle of roughly 10° with the direction defined by Fe3 and Fe4. Hence, the easy axis is not exactly perpendicular to the plane defined by the four iron atoms Fe1, Fe2, Fe3, and Fe4, but makes an angle of about 10° with the normal to this plane as shown in Figure 6.

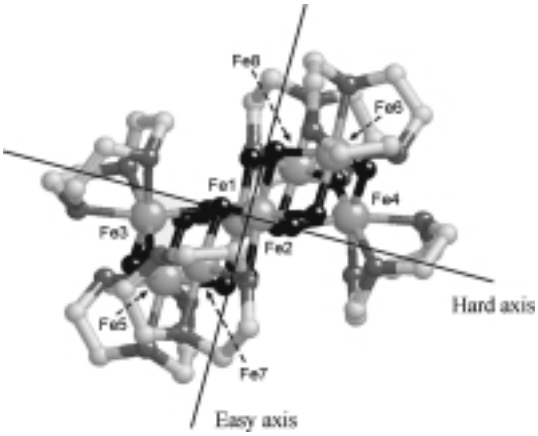

Figure 6. Crystallographic view of the core of the Fe_8 molecule together with the principal axes of the magnetic anisotropy.

These results confirm the expectation that the axis of largest zero-field splitting is roughly orthogonal to the plane of the eight iron(III) ions. They also compare well with previous single-crystal magnetic measurements, which gave an indication that the crystallographic axis a was only 5–10° apart from the easy axis.[36]

Energy levels and quantum-tunneling magnetization (QTM): The present accurate EPR data provide a picture of the splitting of the $S = 10$ ground states, which is displayed in Figure 7, in the two-well formalism that is now commonplace to describe the energy barrier of single-molecule magnets. The energy levels for Mn_{12} are also shown for comparison. It is apparent that for Fe_8 the assumption of essentially degenerate pairs of levels, $\pm M$, is only valid for $|M| > 6$. The higher levels are still quasi degenerate in pairs, except for three states in the middle of the barrier. This is due to the fact that the relatively large transverse anisotropy, given by the contributions of the E, B_4^4, and B_4^2 parameters, results in M not being a good quantum number and an extensive admixture of the states must be expected. This is pictorially shown in Figure 8 for the levels that can be loosely described as $M = \pm 5$ and $M = \pm 6$, respectively. The eigenvectors of the latter are principally

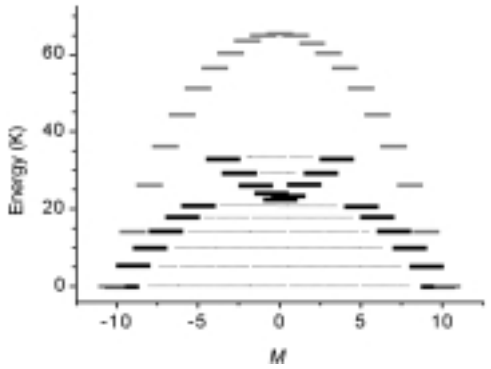

Figure 7. Schematic view of the splitting of the ground $S=10$ state due to the magnetic anisotropy at the origin of the energy barrier for the reversal of the magnetization. The energy levels are calculated for Fe_8 (black) by using the parameters reported in the text and for $Mn_{12}Ac$ (gray) by using the parameters of ref. [31] $D=0.46\ cm^{-1}$, $B_4^0=-2.2\times10^{-5}\ cm^{-1}$, and $B_4^4=4\times10^{-5}\ cm^{-1}$. The abscissa of the energy levels of Fe8 above 20 K is arbitrary being the eigenstates of an admixture of the M states.

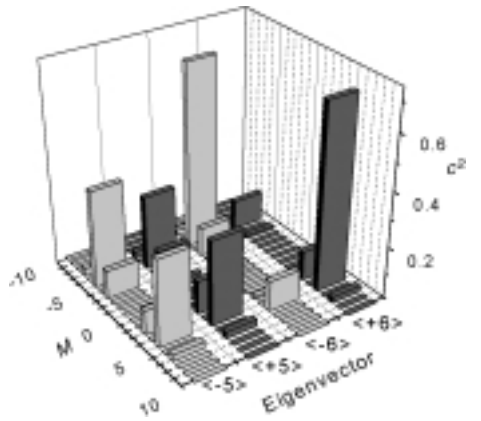

Figure 8. Composition in the M states of the formally ±5, and ±6 states of the ground $S=10$ manifold of Fe_8. In the vertical axis the square of the coefficients of the linear combination are reported.

composed of $M=+6$ and $M=-6$ and are therefore in agreement with the double-well description. On the other hand, the eigenvectors of the former are largely delocalized, and labelling one state as $M=+5$ and the other as $M=-5$ is totally formal. Under these conditions the $\Delta M=\pm1$ rule for the stepwise reorientation of the magnetization simply breaks down and the system does not have to reach the top of the barrier to invert the direction of the magnetization. In fact the top level is not a pure $M=0$ state, but is given by an admixture of many states. Therefore, the $\Delta=|D|S^2$ rule for the estimation of the anisotropy barrier also breaks down.[37] In accord with this view it must be stressed that the Arrhenius law is actually never well obeyed for Fe_8. The behavior of $Mn_{12}Ac$ is different because it has the crystal-imposed symmetry S_4. Under these conditions only the smaller B_4^4 terms induce some admixture of the M states differing by multiples of ±4. Therefore, the $\pm M$ states remain essentially degenerate up to the top of the barrier, the $\Delta=|D|S^2$ rule in this case holds, and an Arrhenius behavior of the relaxation time of the magnetization of $Mn_{12}Ac$ is observed.[38] In both cases the first excited state, characterized by $S=9$, is relatively close in energy, and overlap of the states with those arising from the ground $S=10$ is expected. However, only the transverse anisotropy terms have some effect on the mixing of the states of different S, and this mixing reflects small changes in resonance fields without major alteration to the diagram depicted in Figure 7.

Confirmation of the fact that in the presence of sizeable transverse anisotropy the $\Delta=|D|S^2$ rule does not hold is dramatically proved by the low-temperature dynamics of the magnetization of $[Mn^{III}(dbm)_3]$, in which dbm = 1,3-diphenyl-1,3-propanedionate. This simple compound with $S=2$ has been found by HF-EPR spectra to have $D=-4.35\ cm^{-1}$ and $E/D=0.060$.[39] Using the $\Delta=|D|S^2$ rule, we calculated a barrier of 25.0 K, which would suggest slow relaxation of the magnetization with time characteristically exceeding 1 s below about 1.5 K (on the assumption that the pre-exponential factor in the Arrhenius law $\tau_0=1\times10^{-7}$, which is in agreement with the value of $Mn_{12}Ac$). However, we performed alternating current susceptibility measurements to as low as 0.3 K and did not find any evidence of slow relaxation of the magnetization. The interpretation that we give is that the $M=-2$ to $M=+2$ transition probability is large enough, due to low symmetry effects, to allow direct inversion of the magnetization. This also clarifies the meaning of the conditions we stated above for the observation of slow relaxation of the magnetization at low temperature. Since the largest transverse anisotropy term is given by the Hamiltonian $H=E(\boldsymbol{S}_x^2-\boldsymbol{S}_y^2)$, which couples states that differ by ±2 in M, only for large values of M will the effect of E be negligible and the states degenerate in pairs. In fact the splitting terms for $\pm M$ will occur at the M level of perturbation. For $M=\pm10$ the E term gives a splitting only at the tenth-order perturbation, whereas for $M=\pm2$ it occurs at the second order.

The presence of sizeable transverse anisotropy not only substantially lowers the barrier for the reorientation of the magnetization, but it also provides the admixing of the $\pm M$ states that is required for the tunneling of the magnetization at low temperature. In fact the direct tunneling in zero field of the magnetization of $Mn_{12}Ac$ has never been observed below 2 K, because the tunnel splitting of the $M=\pm10$ states is exceedingly low ($7.7\times10^{-12}\ cm^{-1}$) and the corresponding relaxation time is extremely long. The most accurate measurements of τ indicate a τ value of about 40 years at 1.5 K for $Mn_{12}Ac$.[40] The transverse anisotropy is much larger in Fe_8. With the parameters obtained here, we calculate a tunnel splitting of the $M=\pm10$ states of $4.9\times10^{-9}\ cm^{-1}$, which is approximately three orders of magnitude larger than in $Mn_{12}Ac$. In agreement with this, a tunneling relaxation time of about 6×10^4 s, which is independent of temperature below 0.36 K, has been experimentally observed.[28]

Dipolar contribution to the magnetic anisotropy: The physical origin of the magnetic anisotropy in iron(III) clusters can be either dipolar or single ion. The former arises from the through-space interaction between the magnetic dipoles prevalently located on the iron ions, and the latter by the contribution of the single ions through their low-symmetry components. Several analyses of these contributions have been performed, with different results.[6, 41] In fact in some cases the dipolar contribution, which is easy to calculate, was found to be in good agreement with the experimental

0947-6539/00/0609-1612 $ 17.50+.50/0 *Chem. Eur. J.* **2000**, *6*, No. 9

anisotropy, while in other cases a single-ion contribution corresponding to up to 75% of the experimental anisotropy had to be included.

The evaluation of the dipolar contribution to the magnetic anisotropy of Fe_8 requires that the wavefunction of the ground $S = 10$ state is known. The temperature dependence of the magnetic susceptibility has been reproduced by using the Heisenberg exchange spin Hamiltonian [Eq. (3)] with the

$$H = \Sigma_{i \neq j} J_{ij} \cdot \boldsymbol{S}_i \cdot \boldsymbol{S}_j \quad (3)$$

irreducible tensor operators approach[42] and assuming D_2 symmetry to reduce the size of the matrices to be diagonalized.[43] A true fitting procedure was not performed; however, the experimental data are well reproduced with the following parameters: $J_{13} = 140\ cm^{-1}$, $J_{12} = 25\ cm^{-1}$, $J_{17} = 18\ cm^{-1}$, and $J_{37} = 41\ cm^{-1}$. In the calculation, the zero-field splitting of the ground state and that of the first excited state, which is an $S = 9$ at about $24.5\ cm^{-1}$, were taken into account.[44] These parameters are slightly different from those reported previously,[43] for which the decrease of χT at low temperature was attributed to an $S = 9$ ground state close to an excited $S = 10$ instead of the presence of magnetic anisotropy. These new parameters compare well with data reported in the literature for μ-oxo and μ-hydroxo Fe^{III} pairs and with the dependence of the J values on the Fe-O-Fe bridge. In fact the smallest J_{18} value is associated with a pair of ions in which the Fe-O-Fe angle is on average 100°, and which is therefore small enough to reduce the extent of the antiferromagnetic coupling.[45–47]

The composition of the wavefunction describing the $S = 10$ ground state has been determined by diagonalizing the $S = 10$ block (6328×6328) and evaluating which spin functions contribute most to the ground state. In order to easily describe the eigenvectors it is necessary to choose a coupling scheme of the individual s_i spins that best corresponds to the spin structure of the ground state. The basis function was chosen according to a recent single-crystal polarized neutron diffraction experiment, which has shown that the spin structure at low temperature is reasonably well described by Figure 1, with Fe3 and Fe4 roughly aligned antiparallel to the remaining iron spins. Therefore, s_3 and s_4 are coupled to give S_{34}, s_1 and s_2 are coupled to give S_{12}, and this intermediate spin is successively coupled to s_5 to give S_{1-5}, and so on up to S_{1-8}, which is eventually coupled to S_{34} to give the total spin state $S_{tot.}$. The ground state is then mainly (ca. 70%) described by the basis function shown in Equation 4 with a further 10% contribution provided by that shown in Equation 5. The remaining 20% is provided by several states with smaller contributions.

$$|S_{34},S_{12},S_{1-5},S_{1-6},S_{1-7},S_{1-8},S_{tot}\rangle = |5,5,7.5,10,12.5,15,10\rangle \quad (4)$$

$$|S_{34},S_{12},S_{1-5},S_{1-6},S_{1-7},S_{1-8},S_{tot}\rangle = |5,5,6.5,9,11.5,14,10\rangle \quad (5)$$

The dipolar contribution to the magnetic anisotropy is described in Equation 6, in which i and j extend over the eight iron spins and $\boldsymbol{S}$ corresponds to the total spin operator. The projection coefficients, d_{ij}, can be calculated by using recurrent formulae of angular momenta coupling,[48] and the interatomic $\boldsymbol{D}_{ij}$ tensors can be expressed in the point dipole approximations as shown in Equation 7.

$$H_{dip} = \boldsymbol{S} \cdot \boldsymbol{D} \cdot \boldsymbol{S} = \boldsymbol{S}(\Sigma_{i<j} \cdot d_{ij} \cdot \boldsymbol{D}_{ij})\boldsymbol{S} \quad (6)$$

$$\boldsymbol{D}_{ij} = \mu_B^2 / R_{ij}^3 (\mathbf{g}_i \cdot \mathbf{g}_j - 3(\mathbf{g}_i \cdot \mathbf{R}_{ij})(\mathbf{R}_{ij} \cdot \mathbf{g}_j)/R_{ij}^2) \quad (7)$$

For the spin wavefunctionthat contributes most to the ground state, we evaluated $D = 0.037\ cm^{-1}$ and $E/D = 0.24$. Neither the sign of the calculated ZFS parameters, nor the magnitude, which is almost one order of magnitude smaller, compares well with the experimental parameters. The calculated intermediate principal axis is oriented approximately along the Fe1–Fe2 direction, as experimentally observed, while the easy axis is at approximately 40° from the perpendicular to the Fe1-Fe2-Fe3-Fe4 average plane. A value of $D = 0.029\ cm^{-1}$ is calculated for the second basis function. Therefore it seems reasonable to conclude that single ion contributions are dominant in determining the magnetic anisotropy of Fe_8. A similar conclusion was previously suggested.[18] These results are similar to those reported for Fe_4,[6] which show how iron(III) may in some cases be quite anisotropic.

Conclusions

The accurate single-crystal EPR analysis of Fe_8 has provided clear indication of the principal axes of the magnetic-anisotropy tensor and of the low-symmetry components of the crystal field. The data clearly show that the barrier concept in single-molecule magnets must be critically considered when the transverse fields are sizeable. Concerning the origin of the magnetic anisotropy in iron(III) clusters, compound Fe_8 shows that single-ion contributions are dominant. Although this is often the case, it is important to remember that in antiferromagnetic rings with six and ten ions the dipolar contributions could completely justify the observed anisotropy.[41] Therefore iron(III) clusters do not easily provide single-molecule magnets by design, because the conditions for large Ising type anisotropy depend very unpredictably on minor features of the coordination environment of the metal ions. Matters are different for Mn_{12} and similar compounds in which the presence of the highly anisotropic manganese(III) ions can give rise to large anisotropy in a rather clearly understandable way.

Acknowledgement

We thank A. Caneschi for providing the Fe_8 crystals, and H. Weihe for providing the program for the simulation of the EPR spectra. The financial support of Italian MURST and of the European TMR program (Contract number: ERBFMGECT950077) is gratefully acknowledged.

[1] Z. M. Sun, C. M. Grant, S. L. Castro, D. N. Hendrickson, G. Christou, *Chem. Commun.* **1998**, 721–722.
[2] S. L. Castro, Z. M. Sun, C. M. Grant, J. C. Bollinger, D. N. Hendrickson, G. Christou, *J. Am. Chem. Soc.* **1998**, *120*, 2365–2375.
[3] S. M. J. Aubin, Z. M. Sun, I. A. Guzei, A. L. Rheingold, G. Christou, D. N. Hendrickson, *Chem. Commun.* **1997**, 2239–2240.

[4] M. Clemente-Leon, H. Soyer, E. Coronado, C. Mingotaud, C. J. Gomez-Garcia, P. Delhaes, *Angew. Chem.* **1998**, *110*, 3053 – 3056; *Angew. Chem. Int. Ed.* **1998**, *37*, 2842 – 2845.
[5] E. K. Brechin, J. Yoo, M. Nakano, J. C. Huffman, D. N. Hendrickson, G. Christou, *Chem. Commun.* **1999**, 783 – 784.
[6] A. L. Barra, A. Caneschi, A. Cornia, F. F. De Biani, D. Gatteschi, C. Sangregorio, R. Sessoli, L. Sorace, *J. Am. Chem. Soc.* **1999**, *121*, 5302 – 5310.
[7] A. H. Morrish, *The Physical Principles of Magnetism*, Wiley, New York, **1966**, p. 360.
[8] R. Sessoli, D. Gatteschi, A. Caneschi, M. A. Novak, *Nature* **1993**, *365*, 141 – 143.
[9] B. Barbara, L. Gunther, *Phys. World* **1999**, *12*, 35 – 39.
[10] Z. M. Sun, D. Ruiz, E. Rumberger, C. D. Incarvito, K. Folting, A. L. Rheingold, G. Christou, D. N. Hendrickson, *Inorg. Chem.* **1998**, *37*, 4758 – 4759.
[11] S. M. J. Aubin, S. Spagna, H. J. Eppley, R. E. Sager, G. Christou, D. N. Hendrickson, *Chem. Commun.* **1998**, 803 – 804.
[12] H. J. Eppley, H.-L. Tsai, N. de Vries, K. Folting, G. Christou, D. N. Hendrickson, *J. Am. Chem. Soc.* **1995**, *117*, 301 – 317.
[13] R. Sessoli, H. L. Tsai, A. R. Schake, S. Wang, J. B. Vincent, K. Folting, D. Gatteschi, G. Christou, D. N. Hendrickson, *J. Am. Chem. Soc.* **1993**, *115*, 1804 – 1816.
[14] A. Caneschi, D. Gatteschi, R. Sessoli, A.-L. Barra, L. C. Brunel, M. Guillot, *J. Am. Chem. Soc.* **1991**, *113*, 5873 – 5874.
[15] G. Aromi, S. M. J. Aubin, M. A. Bolcar, G. Christou, H. J. Eppley, K. Folting, D. N. Hendrickson, J. C. Huffman, R. C. Squire, H. L. Tsai, S. Wang, M. W. Wemple, *Polyhedron* **1998**, *17*, 3005 – 3020.
[16] T. Lis, *Acta Crystallogr. Sect. B* **1980**, *36*, 2042 – 2046.
[17] K. Wieghardt, K. Pohl, I. Jibril, G. Huttner, *Angew. Chem.* **1984**, *96*, 66 – 67; *Angew. Chem. Int. Ed. Engl.* **1984**, *23*, 77 – 78.
[18] A. L. Barra, P. Debrunner, D. Gatteschi, Ch. E. Schulz, R. Sessoli, *Europhys. Lett.* **1996**, *35*, 133 – 138.
[19] T. Mallah, C. Auberger, M. Verdaguer, P. Veillet, *J. Chem. Soc. Chem. Commun.* **1995**, 61 – 62.
[20] A. Scuiller, T. Mallah, M. Verdaguer, A. Nivorozkhin, J.-L. Tholence, P. Veillet, *New J. Chem.* **1996**, *20*, 1 – 8.
[21] S. M. J. Aubin, N. R. Dilley, L. Pardi, J. Krzystek, M. W. Wemple, L. C. Brunel, M. B. Maple, G. Christou, D. N. Hendrickson, *J. Am. Chem. Soc.* **1998**, *120*, 4991 – 5004.
[22] B. Pilawa, M. T. Kelemen, S. Wanka, A. Geisselmann, A. L. Barra, *Europhys. Lett.* **1998**, *43*, 7 – 12.
[23] A. L. Barra, A. Caneschi, D. Gatteschi, D. P. Goldberg, R. Sessoli, *J. Solid State Chem.* **1999**, *145*, 484 – 487.
[24] L. Thomas, F. Lionti, R. Ballou, D. Gatteschi, R. Sessoli, B. Barbara, *Nature* **1996**, *383*, 145 – 147.
[25] J. R. Friedman, M. P. Sarachik, J. Tejada, R. Ziolo, *Phys. Rev. Lett.* **1996**, *76*, 3830 – 3833.
[26] J. Villain, F. Hartman-Boutron, R. Sessoli, A. Rettori, *Europhys. Lett.* **1994**, *27*, 159 – 164.
[27] R. Caciuffo, G. Amoretti, A. Murani, R. Sessoli, A. Caneschi, D. Gatteschi, *Phys. Rev. Lett.* **1998**, *81*, 4744 – 4747.
[28] C. Sangregorio, T. Ohm, C. Paulsen, R. Sessoli, D. Gatteschi, *Phys. Rev. Lett.* **1997**, *78*, 4645 – 4648.
[29] W. Wernsdorfer, R. Sessoli, *Science* **1999**, *284*, 133 – 135.
[30] A. L. Barra, L. C. Brunel, D. Gatteschi, L. Pardi, R. Sessoli, *Acc. Chem. Res.* **1998**, *31*, 460 – 466.
[31] A. L. Barra, D. Gatteschi, R. Sessoli, *Phys. Rev. B* **1997**, *56*, 8192 – 8198.
[32] F. Muller, M. A. Hopkins, N. Coron, M. Grynberg, L. C. Brunel, G. Martinez, *Rev. Sci. Instrum.* **1989**, *60*, 3681 – 3684.
[33] J. Glerup, H. Weihe, *Acta Chem. Scand.* **1991**, 444 – 448.
[34] C. J. H. Jacobsen, E. Pedersen, J. Villadsen, H. Weihe, *Inorg. Chem.* **1993**, *32*, 1216 – 1221.
[35] The labelling of iron atoms is consistent to that of ref. [49].
[36] T. Ohm, PhD Thesis, Université Joseph Fourier – Grenoble 1, **1998**.
[37] J. R. Friedman, *Phys. Rev. B* **1998**, *57*, 10291 – 10294.
[38] M. A. Novak, R. Sessoli, *Quantum Tunneling of Magnetization-QTM'94*, Kluwer Academic, **1995**, pp. 171 – 188.
[39] A. L. Barra, D. Gatteschi, R. Sessoli, G. L. Abbati, A. Cornia, A. C. Fabretti, M. G. Uytterhoeven, *Angew. Chem.* **1997**, *109*, 2423 – 2426; *Angew. Chem. Int. Ed. Engl.* **1997**, *36*, 2329 – 2331.
[40] L. Thomas, B. Barbara, A. Caneschi, unpublished results.
[41] A. Cornia, M. Affronte, A. G. M. Jansen, G. L. Abbati, D. Gatteschi, *Angew. Chem.* **1999**, *111*, 2409 – 2411; *Angew. Chem. Int. Ed.* **1999**, *38*, 2264 – 2266.
[42] D. Gatteschi, L. Pardi, *Gazz. Chim. Ital.* **1993**, *123*, 231 – 240.
[43] C. Delfs, D. Gatteschi, L. Pardi, R. Sessoli, K. Wieghardt, D. Hanke, *Inorg. Chem.* **1993**, *32*3, 99 – 103.
[44] For the first two excited states the same D value as for the $S = 10$ ground state has been assumed.
[45] F. Le Gall, F. F. de Biani, A. Caneschi, P. Cinelli, A. Cornia, A. C. Fabretti, D. Gatteschi, *Inorg. Chim. Acta* **1997**, *262*, 123 – 132.
[46] A. Caneschi, F. F. De Biani, L. Kloo, P. Zanello, *Int. J. Quantum Chem.* **1999**, *72*, 61 – 71.
[47] H. Weihe, H. U. Guedel, *J. Am. Chem. Soc.* **1997**, 6539 – 6543.
[48] A. Bencini, D. Gatteschi, *EPR of Exchange Coupled Systems*, Springer, Berlin, **1990**.
[49] Y. Pontillon, A. Caneschi, D. Gatteschi, R. Sessoli, E. Ressouche, J. Schweizer, E. Lelievre-Berna, *J. Am. Chem. Soc.* **1999**, *121*, 5342 – 5343.

Received: August 30, 1999 [F2007]

  0947-6539/00/0609-1614 $ 17.50+.50/0